Supporting Information

Preparation of α_1- and α_2-isomers of Mono-Ru-substituted Dawson-type Phosphotungstates with an Aqua Ligand and comparison of their Redox Potentials, Catalytic Activities, and Thermal stabilities with Keggin-type derivatives

Kensuke Nishiki,[a] Naoya Umehara,[a] Yusuke Kadota,[a] Xavier López,[b] Josep M. Poblet,[b] Charyle Ayingone Mezui,[c] Anne-Lucie Teillout,[c] Israël M. Mbomekalle,[c] Pedro de Oliveira,[e] Mayumi Miyamoto,[a] Tsuneji Sano,[a] and Masahiro Sadakane,[a, d]*

[a] Department of Applied Chemistry, Graduate School of Engineering, Hiroshima University, 1-4-1 Kagamiyama, Higashi-Hiroshima, 739-8527, Japan. Fax: +81 82 424 5494; Tel: +81 82 424 4456; E-mail: sadakane09@hiroshima-u.ac.jp

[b] Departament de Química Física i Inorgànica, Universitat Rovira i Virgili, Marcel·lí Domingo s/n, 43007 Tarragona, Spain

[c] Laboratoire de Chimie-Physique, Université Paris-Sud, UMR 8000 CNRS, Orsay F-91405, France

[d] PRESTO, Japan Science and Technology Agency (JST), 4-1-8 Honcho, Kawaguchi, 332-0012, Japan

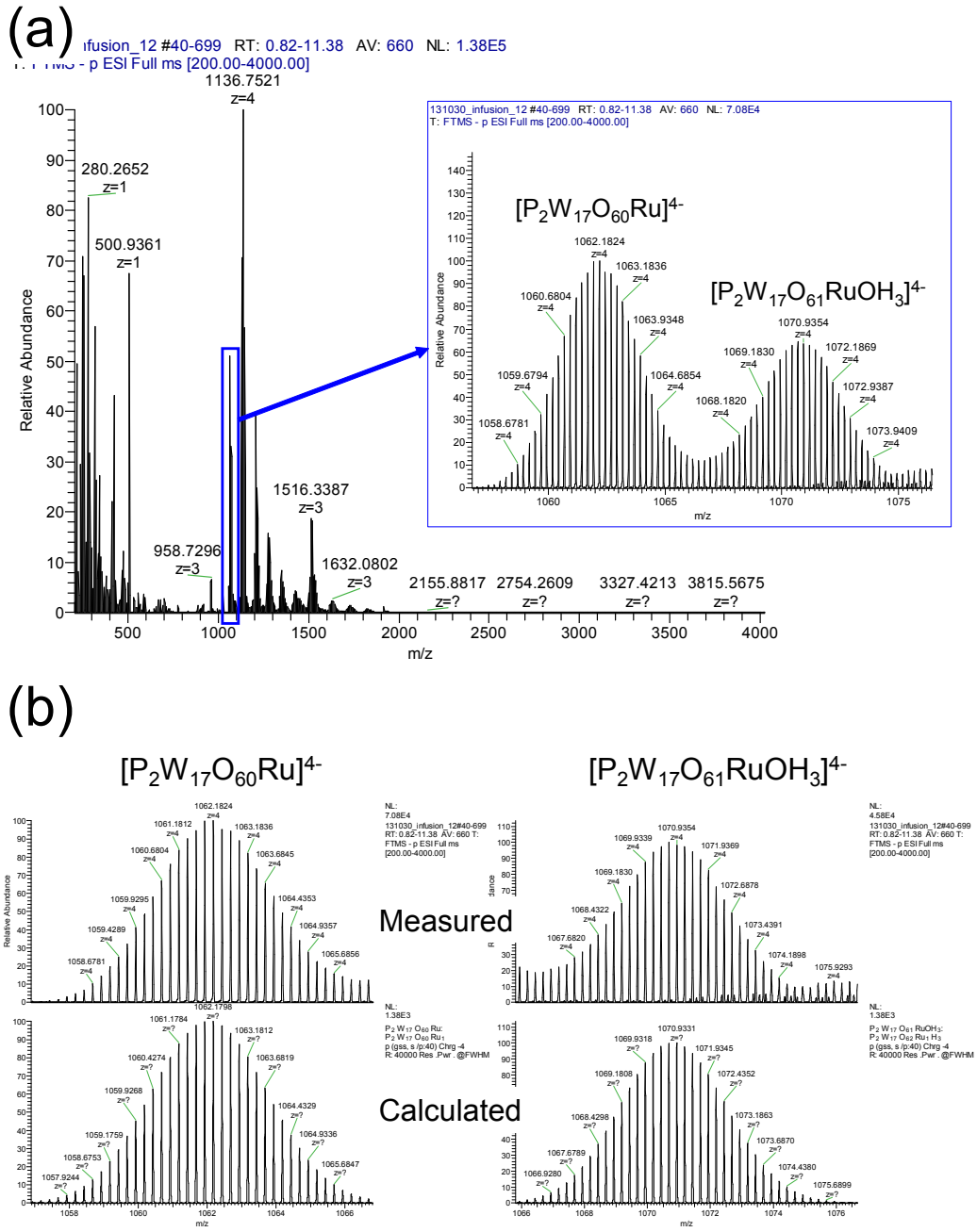

Figure S1. ESI-MS spectroscopy of (a) and (b) $K_7[\alpha_1\text{-}P_2W_{17}O_{61}Ru^{III}(H_2O)]$ (**α_1-RuH$_2$O**), (c) and (d) $K_7[\alpha_2\text{-}P_2W_{17}O_{61}Ru^{III}(H_2O)]$ (**α_2-RuH$_2$O**).

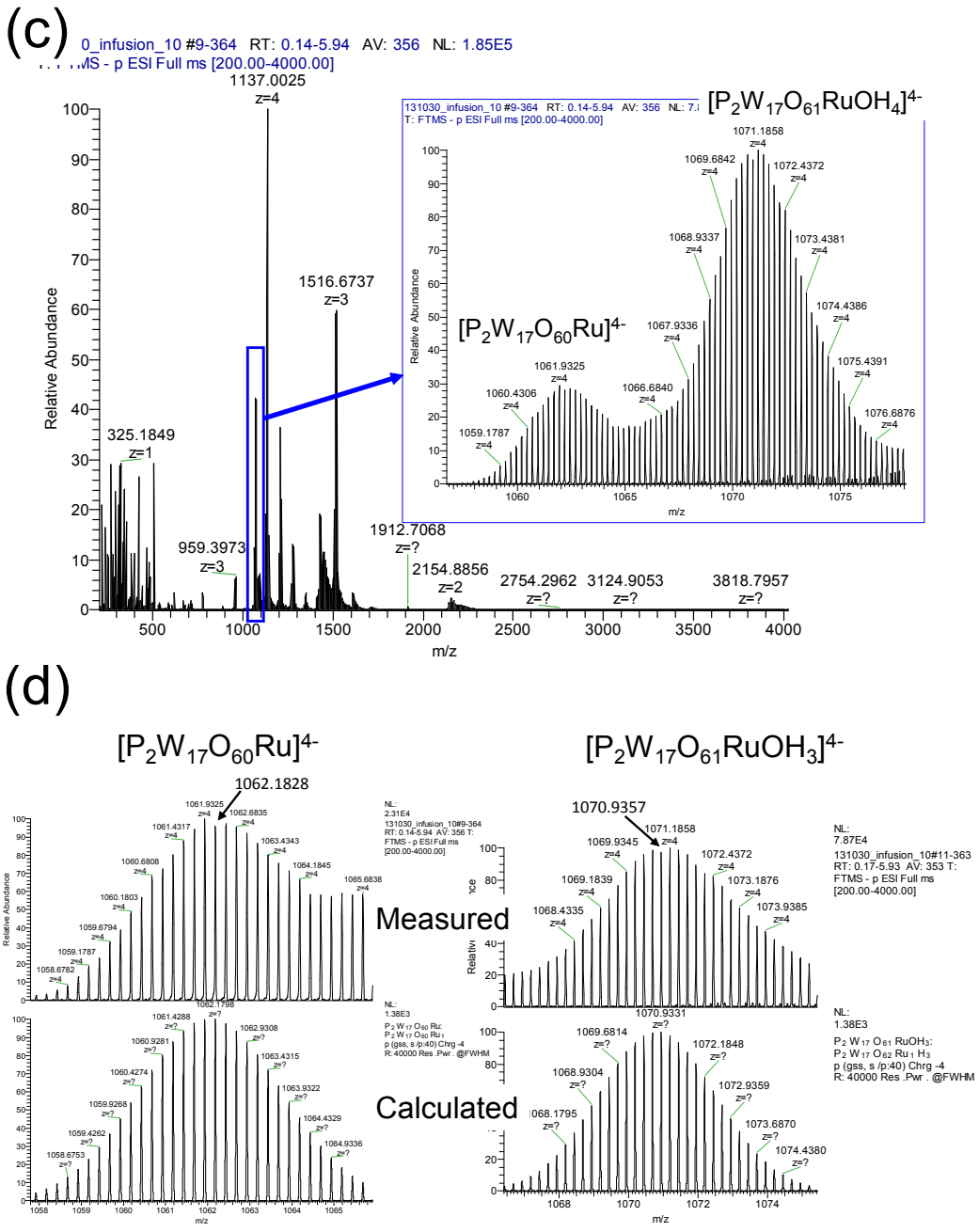

Figure S1. Continued.

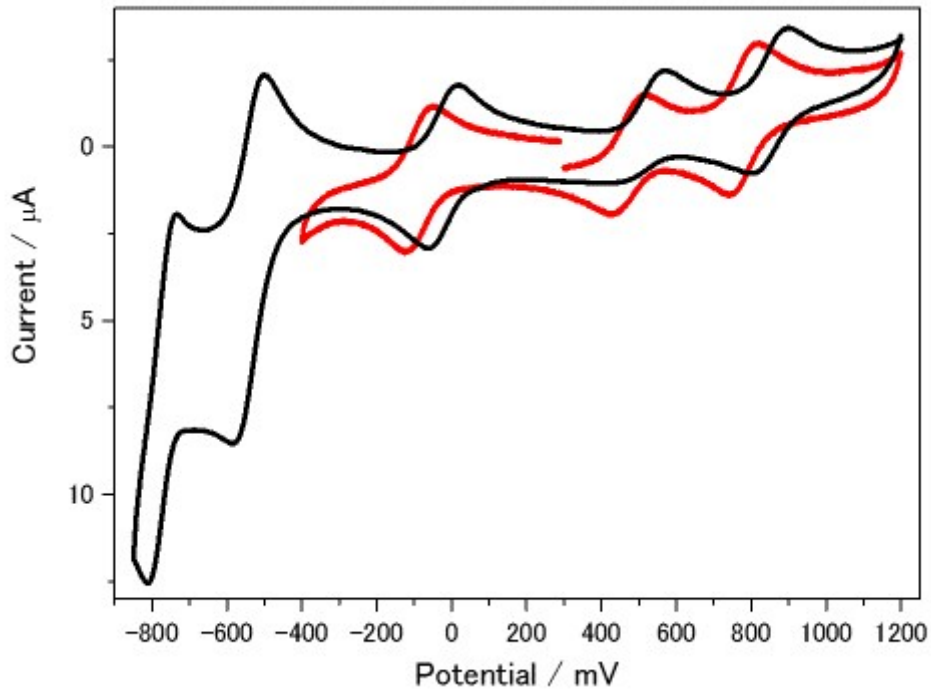

Figure S2. Cyclic voltammograms of the isolated brown solids, (black line) $K_7[\alpha_1\text{-}P_2W_{17}O_{61}Ru^{III}(H_2O)]$ (**α_1-RuH$_2$O**) and (red line) $K_7[\alpha_2\text{-}P_2W_{17}O_{61}Ru^{III}(H_2O)]$ (**α_2-RuH$_2$O**). Cyclic voltammetry was performed in 0.5 M KH_2PO_4 aqueous solutions (pH ca. 4.3). POM concentration: 1.0×10^{-3} M. Scan rate: 25 mV·s^{-1}.

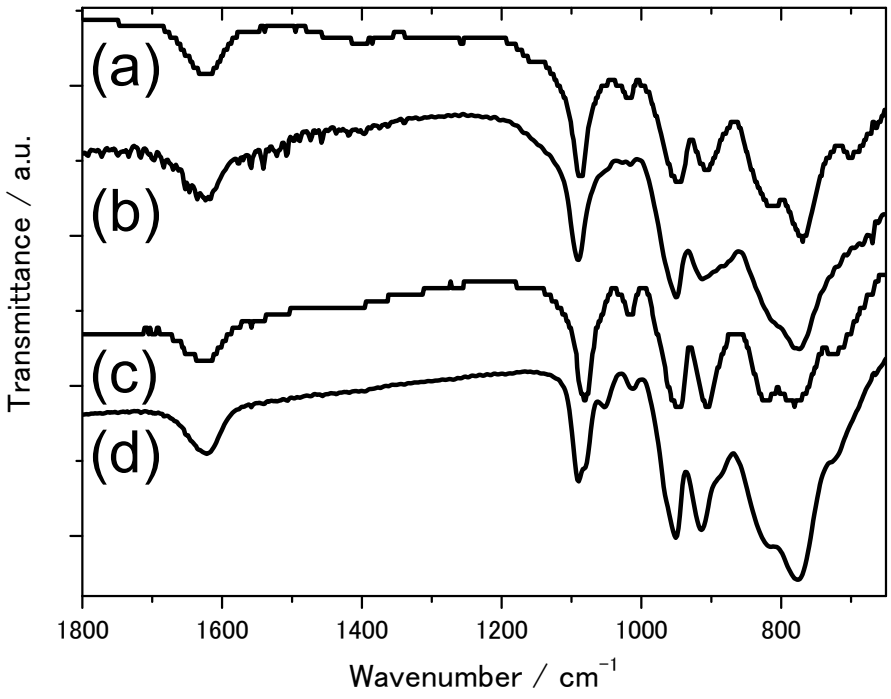

Figure S3. IR spectra of (a) $K_8[\alpha_1\text{-}P_2W_{17}O_{61}Ru^{II}(DMSO)]$ (**α_1-RuDMSO**), (b) the brown solid, $K_7[\alpha_1\text{-}P_2W_{17}O_{61}Ru^{III}(H_2O)]$ (**α_1-RuH_2O**), obtained after reaction of $K_8[\alpha_1\text{-}P_2W_{17}O_{61}Ru^{II}(DMSO)]$ (**α_1-RuDMSO**) in H_2O, (c) $K_8[\alpha_2\text{-}P_2W_{17}O_{61}Ru^{II}(DMSO)]$ (**α_2-RuDMSO**), and (d) the brown solid $K_7[\alpha_2\text{-}P_2W_{17}O_{61}Ru^{III}(H_2O)]$ (**α_2-RuH_2O**), obtained after reaction of $K_8[\alpha_2\text{-}P_2W_{17}O_{61}Ru^{II}(DMSO)]$ (**α_2-RuDMSO**) in H_2O.

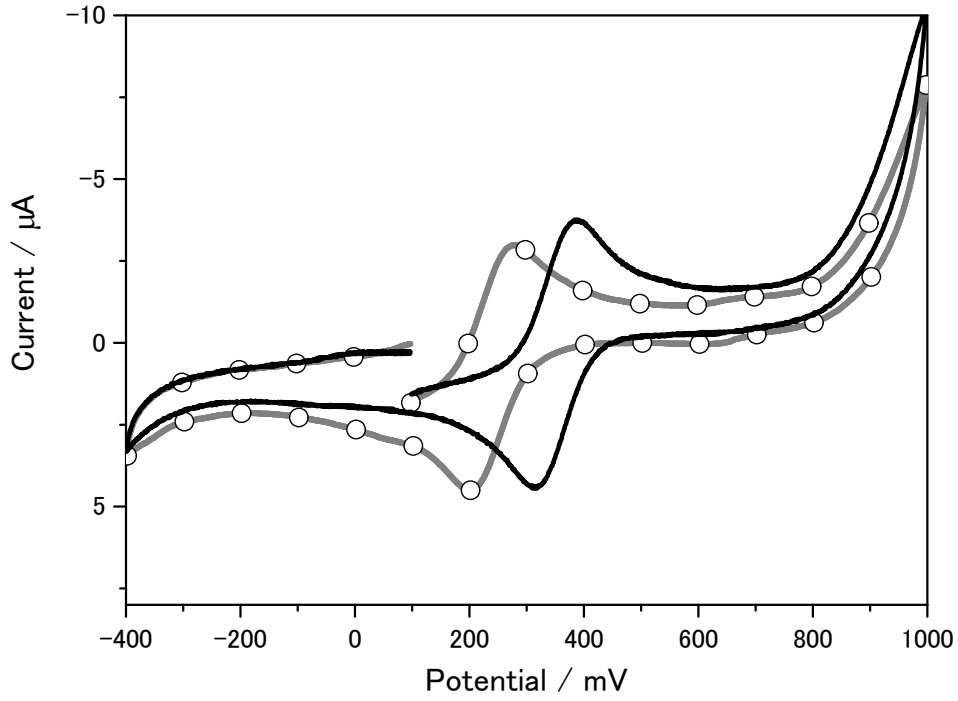

Figure S4. Cyclic voltammograms of re-generated [α_1- and α_2-$P_2W_{17}O_{61}Ru^{III}(DMSO)]^{7-}$ complexes. (black line) the reaction mixture obtained after reaction of [α_1-$P_2W_{17}O_{61}Ru(H_2O)]^{7-}$ and DMSO in water at 80 ºC for 4 days. (grey line with open circles) the reaction mixture obtained after reaction of [α_2-$P_2W_{17}O_{61}Ru(H_2O)]^{7-}$ and DMSO in water at 80 ºC for 4 days. The reaction mixture (0.2 mL) was diluted with 0.54 M KH_2PO_4 (2.8 mL) to obtain a solution containing ca. 1.0 mM of Ru and 0.5 M KH_2PO_4 (pH 4.3).

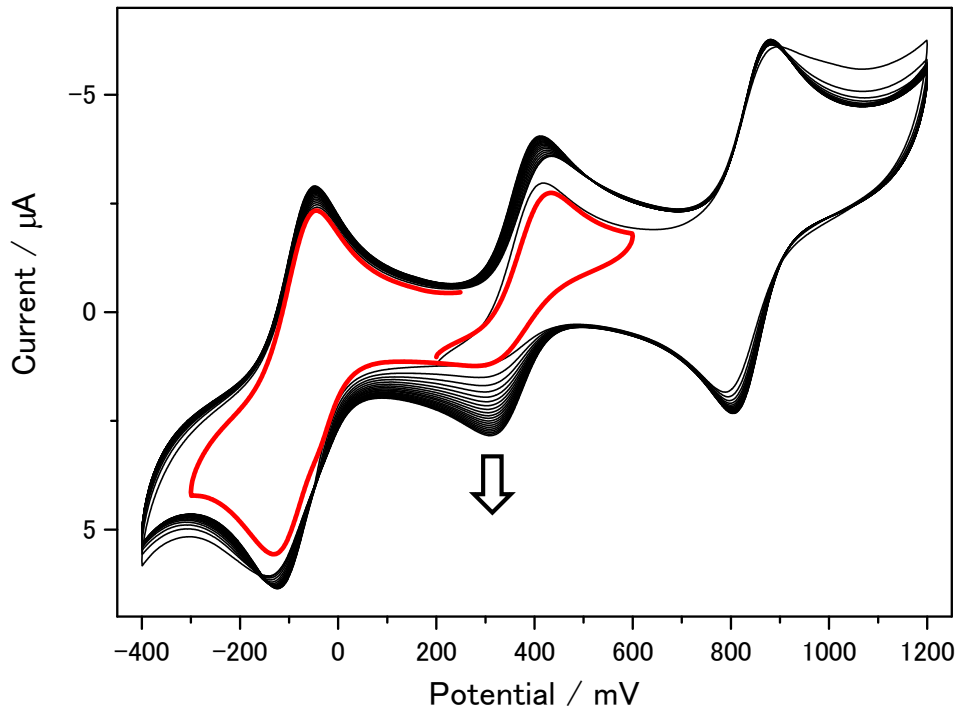

Figure S5. Cyclic voltammograms of $K_7[\alpha_1\text{-}P_2W_{17}O_{61}Ru^{III}(H_2O)]$ (**α_1-RuH$_2$O**) in Britton-Robinson buffer with 0.5 M $NaNO_3$ solution (pH 6.0). (red line) potential window was between 600 mV and -300 mV. (black line) scans between 1200 mV and -400 mV were continually repeated 21 times. Potential scan was started from 200 mV to a positive direction.

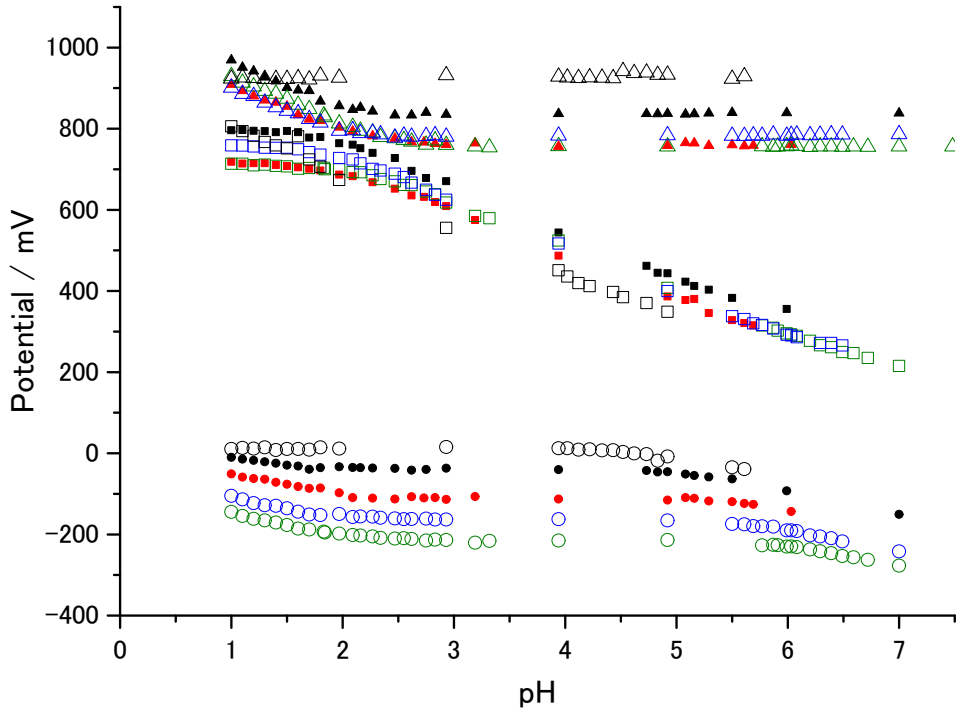

Figure S6. Pourbaix diagram (redox potentials against pH of the solution) of (closed black circles) **α_1-RuH$_2$O**, (closed red circles) **α_2-RuH$_2$O**, (open green circles) $[SiW_{11}O_{39}Ru(H_2O)]^{n-}$, (open blue circles) $[GeW_{11}O_{39}Ru(H_2O)]^{n-}$, and (open black circles) $[PW_{11}O_{39}Ru(H_2O)]^{n-}$. Britton-Robinson buffer (0.2 M NaOH was added to a solution containing CH_3CO_2H (0.04 M), H_3PO_4 (0.04 M), and $B(OH)_3$ (0.04 M)) with 0.5 M $NaNO_3$ for pH range of 1.8-7.0 and 0.5 M $NaHSO_4$ + 0.5 M H_2SO_4 for pH less than 1.8.

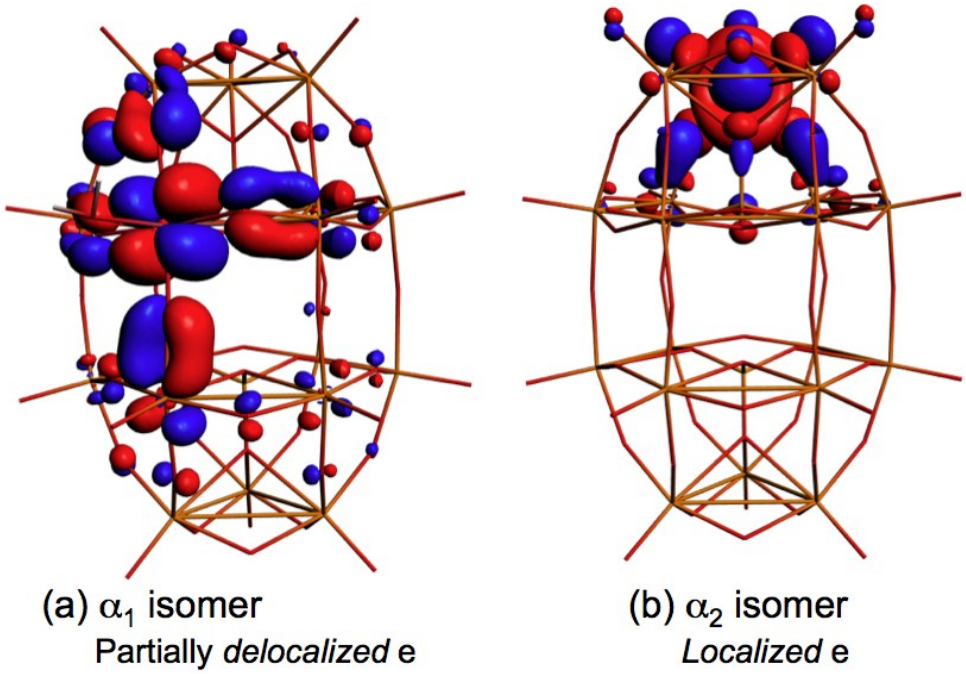

Figure S7. Highest occupied molecular orbital (HOMO), corresponding to the mono-occupied orbital in Figure 8, for (a) α_1-$P_2W_{17}Ru(III)$, side view, and (b) α_2-$P_2W_{17}Ru(III)$, top view. In both cases, the orbital has majority of Ru character.

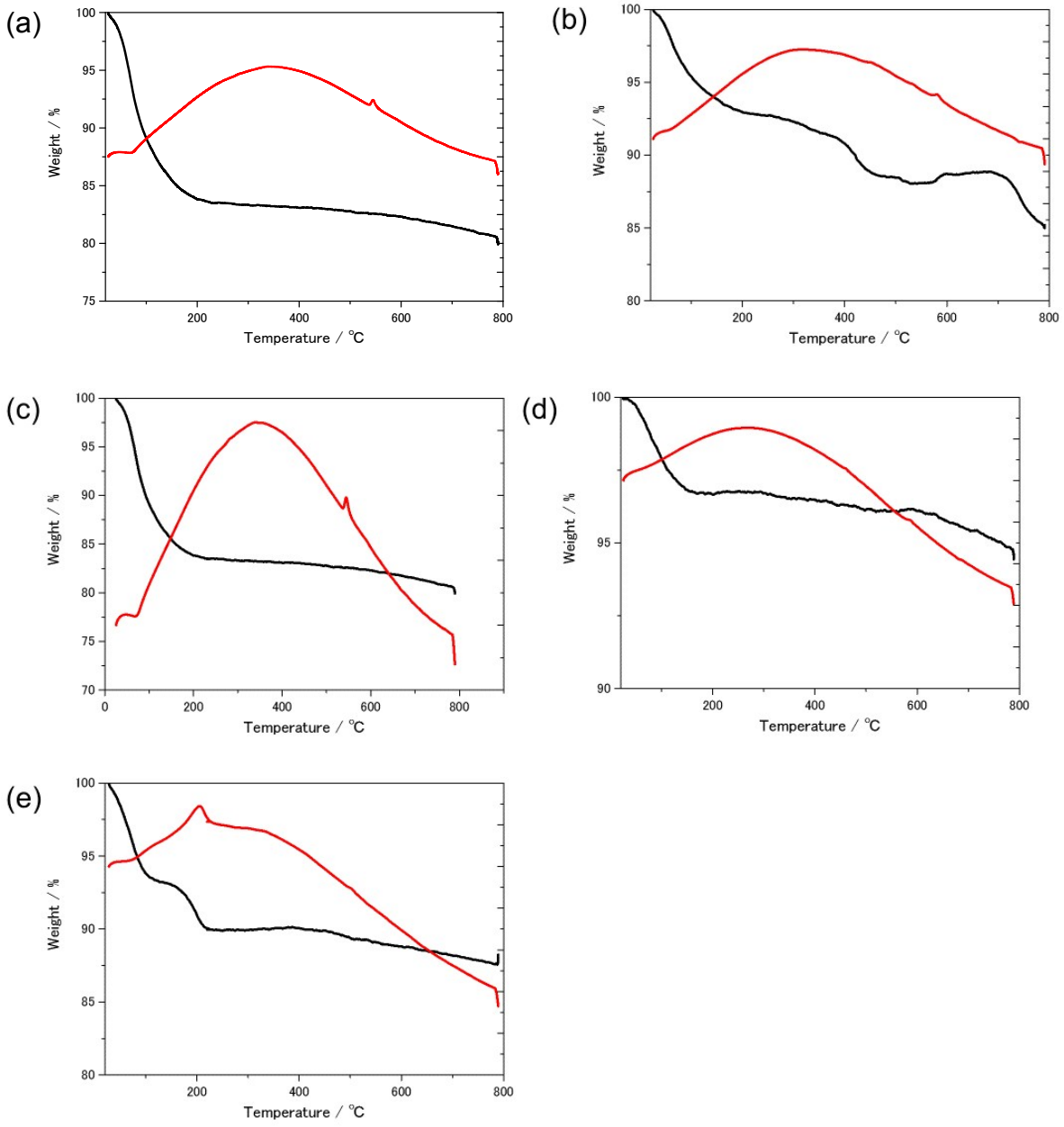

Figure S8. TG-DTA of (a) $K_7[\alpha_1\text{-}P_2W_{17}O_{61}Ru^{III}(H_2O)]$ (**α_1-RuH$_2$O**), (b) $K_7[\alpha_2\text{-}P_2W_{17}O_{61}Ru^{III}(H_2O)]$ (**α_2-RuH$_2$O**), (c) $K_5[SiW_{11}O_{39}Ru(H_2O)]$, (d) $K_5[GeW_{11}O_{39}Ru(H_2O)]$, and (e) $Cs_4[PW_{11}O_{39}Ru(H_2O)]$.

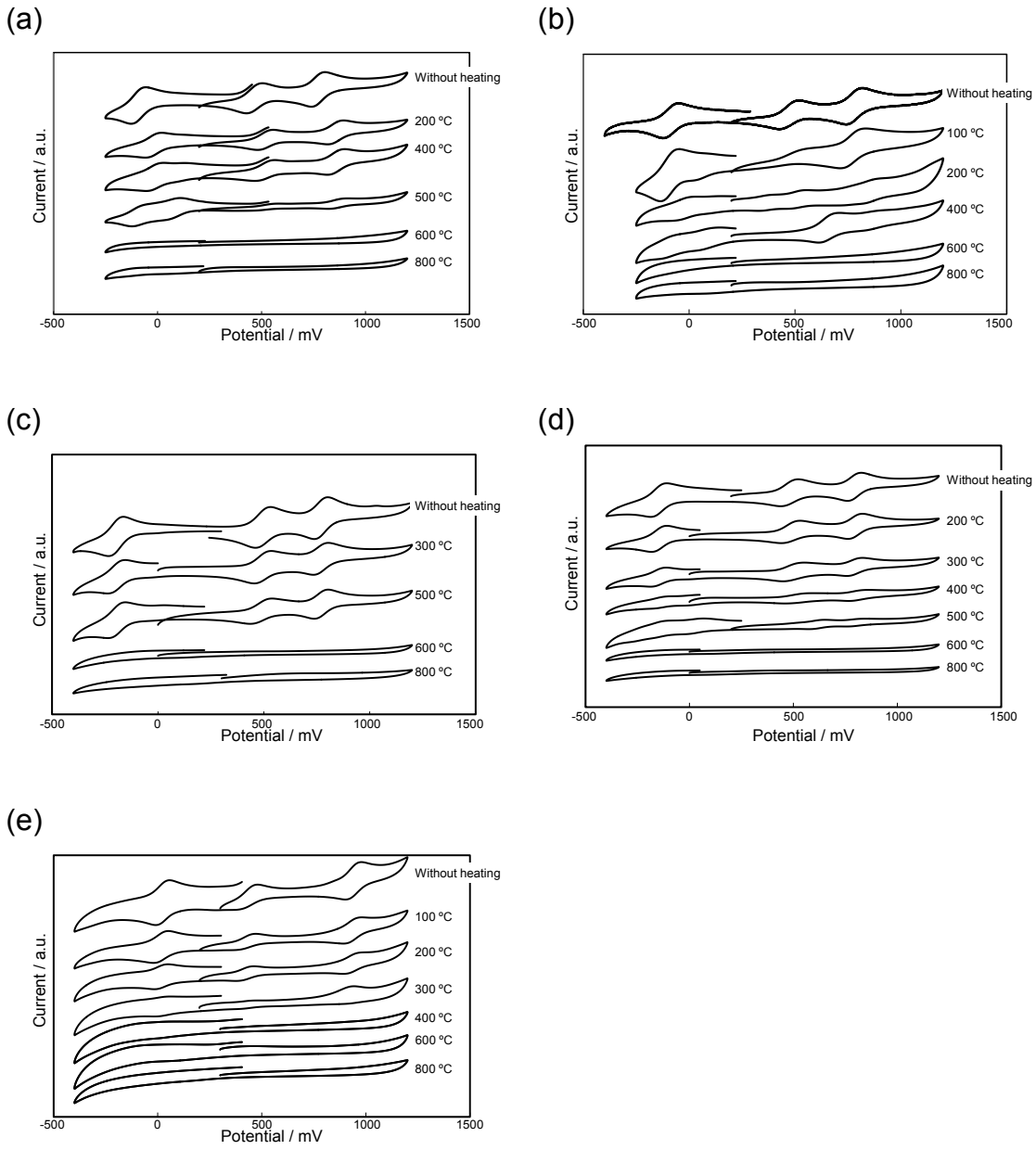

Figure S9. Cyclic voltammograms of (a) $K_7[\alpha_1\text{-}P_2W_{17}O_{61}Ru^{III}(H_2O)]$ (**α_1-RuH$_2$O**), (b) $K_7[\alpha_2\text{-}P_2W_{17}O_{61}Ru^{III}(H_2O)]$ (**α_2-RuH$_2$O**), (c) $K_5[SiW_{11}O_{39}Ru(H_2O)]$, (d) $K_5[GeW_{11}O_{39}Ru(H_2O)]$, and (e) $Cs_4[PW_{11}O_{39}Ru(H_2O)]$ before heating and heating at several temperatures. Samples were heating using TG-DTA apparatus with heating rate of 10 ºC·min^{-1}. Samples (ca. 1 mM of Ru) were dissolved in 0.5 M KH_2PO_4 (pH ca. 4.2).